

Measurement of the neutron detection efficiency of a 80% absorber - 20% scintillating fibers calorimeter.

M. Anelli^a, S. Bertolucci^a, C. Bini^{*,b,c}, P. Branchini^d, G. Corradi^a,
 C. Curceanu^a, G. De Zorzi^{b,c}, A. Di Domenico^{b,c}, B. Di Micco^{e,d}, A. Ferrari^f,
 S. Fiore^{b,c}, P. Gauzzi^{*,b,c}, S. Giovannella^a, F. Happacher^a, M. Iliescu^{a,g},
 A. Lucà^a, M. Martini^a, S. Miscetti^a, F. Nguyen^{e,d}, A. Passeri^d,
 A. V. Prokofiev^h, I. Sarra^a, B. Sciascia^a, F. Sirghi^{a,g}, D. Tagnani^a

^aLaboratori Nazionali di Frascati dell'INFN, Via E.Fermi 40, I-00044 Frascati, Italy.

^bDipartimento di Fisica, Sapienza Università di Roma, P.le A.Moro, 2 I-00185 Roma, Italy.

^cINFN Sezione di Roma, P.le A.Moro, 2 I-00185 Roma, Italy.

^dINFN Sezione di Roma Tre, Via della Vasca Navale, 84 I-00146 Roma, Italy.

^eDipartimento di Fisica dell'Università "Roma Tre", Via della Vasca Navale, 84 I-00146 Roma, Italy.

^fInstitute of Safety Research and Institute of Radiation Physics, Forschungszentrum Dresden-Rossendorf, PF 510119, 01314 Dresden, Germany.

^g"Horia Hulubei" National Institute of Physics and Nuclear Engineering, Str. Atomistilor no. 407, P.O. Box MG-6 Bucharest-Magurele, Romania.

^hThe Svedberg Laboratory, Uppsala University, Box 533, S-751 21 Uppsala, Sweden.

Abstract

The neutron detection efficiency of a sampling calorimeter made of 1 mm diameter scintillating fibers embedded in a lead/bismuth structure has been measured at the neutron beam of The Svedberg Laboratory at Uppsala. A significant enhancement of the detection efficiency with respect to a bulk organic scintillator detector with the same thickness is observed.

Key words: Neutron detection, Calorimetry, Scintillating fibers

1. Introduction

Neutrons of kinetic energies ranging between few and few hundreds MeV are normally detected using organic scintillators, the high concentration of hydrogen atoms providing the proton target where the neutrons are elastically scattered. In this energy range the efficiency of scintillator slabs smoothly depends on the neutron kinetic energies and is typically of 1% for every cm of scintillator thickness [1].

It has been suggested that the insertion of a high Z material in a structure of

*Corresponding author, Dipartimento di Fisica, Sapienza Università di Roma, P.le A.Moro, 2 I-00185 Roma, Italy; Tel. +390649914266, Fax +39064957697

Email addresses: cesare.bini@roma1.infn.it (C. Bini), paolo.gauzzi@roma1.infn.it (P. Gauzzi)

organic scintillators could significantly enhance the neutron detection efficiency, due to the abundant production of secondary particles in inelastic interactions of the neutrons with the high Z material [2]. Compact detectors for neutrons of these energies are required by the experiments proposed at the e^+e^- collider DAΦNE of the Frascati Laboratories, aiming to measure the neutron time-like form factors [3] and the low energy charged kaon interactions on nuclei [4]. In view of these projects, recently the neutron detection efficiency of a lead-scintillating fibers calorimeter where the percentage in volume of the active medium is about 50% (the KLOE calorimeter [5]) has been measured. An efficiency enhancement of a factor about 3 has been measured with respect to a NE-110 bulk scintillator with an equivalent scintillator thickness exposed to the same beam [6].

In this paper we present the results of the experimental study of the response and of the detection efficiency to neutrons of a different heterogeneous calorimeter module which is still based on scintillating fibers but with a lower percentage of active medium, about 20% in volume. Note that lead scintillating fibers calorimeters with this percentage of scintillator, allow also to obtain the best compensation for hadron calorimetry [7].

2. The calorimeter

The calorimeter module [8], 32 cm in length and (7.5×7.5) cm² in cross-section was built with a fusion technique: a high density alloy (9.9 g/cm³; alloy composition: 52.5% Bi + 32.0% Pb + 15.5% Sn, in weight) with low temperature melting point encloses an array of thin stainless steel tubes 100 μm thick, each containing a 1 mm diameter scintillating fiber. The fibers, Kuraray SCSF-81, run parallel along the module length and are positioned in the transverse plane at the vertices of squares of 2.1 mm side. The overall structure is characterized by a scintillator percentage in volume of 19.5%. At each module edge the fibers are grouped together in two bundles directly connected to Hamamatsu fine-mesh R5946 1.5' photomultiplier tubes (PM). The gains of the four PMs have been adjusted in such a way to have the same response to a minimum ionizing particle (mip) for each channel. Each PM signal is split and discriminated: charge and time distributions are obtained through the KLOE ADC and TDC modules [5]. The analog sums of the two signals from each side of the module provide the auto-trigger: the trigger requires both analog sums to be larger than a given threshold V_{th} that can be varied in a wide range.

In order to compare the efficiency extracted from these measurements with those from different detectors, we express the threshold in equivalent electron energy E_{th} (MeV el.eq.). The correspondence between V_{th} and E_{th} is given by:

$$E_{th}(\text{MeV el.eq.}) = V_{th}(\text{mV}) \times \frac{\lambda(\text{count/mV})\delta E(\text{MeV})}{MIP(\text{count})(e/mip)} \quad (1)$$

Here λ is the conversion factor from ADC counts to mV; MIP is the peak value in ADC counts mips crossing the calorimeter with the same direction of

the neutrons. This mip sample has been obtained in a cosmic ray run with the calorimeter rotated by 90° around the fiber direction triggered by two small scintillators. $\delta E = 80$ MeV is the calculated energy release by a mip in the calorimeter module; (e/mip) is the ratio between the response to a 80 MeV electron and to a mip [7]. Our (e/mip) estimate is based on the cosmic ray run (see above) compared to runs with electrons at the Beam Test Facility (BTF) of the Frascati Laboratories. We obtain a value of (e/mip) compatible with 1 within 15%. Due to the small longitudinal size of our calorimeter, we correct for the leakage affecting the electron energy measurement. On the other hand, a value of $(e/mip) = 0.72 \pm 0.03$ is obtained in Ref.[9] for a scintillating fiber calorimeter with a filling factor of about 20% but with a different absorber composition and for much higher energies (above 4 GeV). In the following, we consider the interval between the two values of (e/mip) as a systematic uncertainties of the absolute electron equivalent energy scale.

The threshold can also be expressed in number of photo-electrons (p.e.) using the measured values of the PM gains. We obtain a correspondence approximately of 1 p.e. / MeV el.eq. We have explored a threshold range between 6 and 120 MeV per side.

3. Experimental set-up

We have exposed the calorimeter module to the neutron beam of The Svedberg Laboratory (TSL) in Uppsala University [10]. A proton beam of 178.7 MeV kinetic energy is sent to a 23.5 mm thick ^7Li target at a frequency of about 20 MHz. A bending magnet and an iron collimator block about 1 m long with a 2 cm diameter cylindrical hole allow to select a neutron beam with negligible contamination. Fig.1 shows the experimental layout.

The kinetic energy spectrum of the neutrons emerging from the hole is shown in Fig.2. It is characterized by the quasi-elastic peak at 174 MeV and by a tail extending to very low energies, the integral of the quasi-elastic peak being about 40% of the total spectrum. The neutron flux at the collimator exit is measured online with an Ionization Chamber Monitor (ICM). The ICM measurements are periodically calibrated with another monitor based on Thin-Film Breakdown Counter in order to obtain the absolute neutron rate, that is provided with an accuracy of about 15%. The beam has two components: a bulk component with a Gaussian shape and a larger halo which is not fully accounted for by the ICM. Therefore the total neutron rate has to be corrected in order to properly normalize the absolute efficiency measurement.

A 20 MHz signal synchronous with the proton beam is provided to the experiment and is used to strobe the calorimeter trigger signal thus acting as start signal for the neutron time of flight measurement.

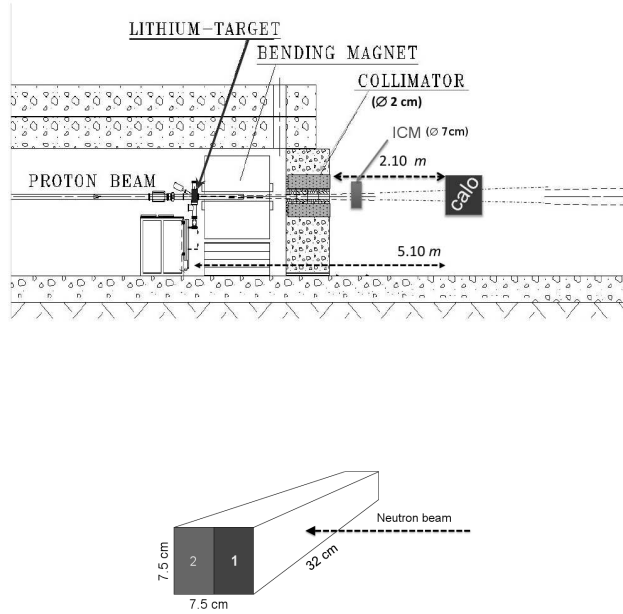


Figure 1: TSL experimental lay-out: (top) calorimeter position on the TSL beam-line; (bottom) enlarged view of the calorimeter.

4. Results and discussion

Charge and time spectra of the calorimeter are shown in Fig.3 for a typical run with $E_{th}=36$ MeV el.eq.. Continuous charge spectra clearly cut at the threshold value and characterized by a tail extending up to the ADC saturation value corresponding to about 450 MeV el.eq. are obtained. The time spectrum is correlated to the neutron kinetic energy spectrum, the large peak corresponding to the 174 MeV neutron peak and the large time tail corresponding to lower kinetic energies. The time spectrum is used to estimate the efficiency dependence on the neutron energy as shown in the following. However, such correlation is reduced by the time resolution and, to a minor extent, by a small amount of re-phasing effect due to the 20 MHz structure of the start signal.

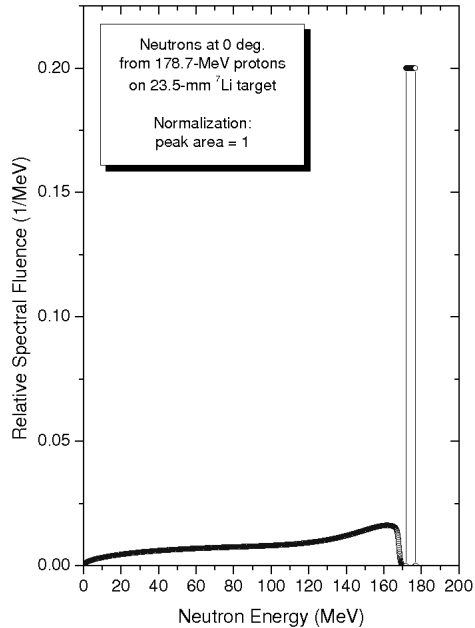


Figure 2: TSL expected neutron kinetic energy spectrum out of the collimator.

This latter effect results in a fixed time spectrum width of 45 ns, and implies that the time of flight of very low energy neutrons can overlap with the one of 174 MeV neutrons.

The overall detection efficiency of the calorimeter is defined as:

$$\epsilon = \frac{r_{calo}}{r_{ICM}} \times \frac{f_{ICM}}{A} \quad (2)$$

where:

- r_{calo} is the calorimeter trigger rate, the accidental trigger rate being negligible;
- r_{ICM} is the neutron rate measured by ICM;
- f_{ICM} is the ratio between the integral of the bulk neutron distribution and the overall neutron rate impinging on the calorimeter;
- A is the acceptance of the calorimeter for bulk neutrons.

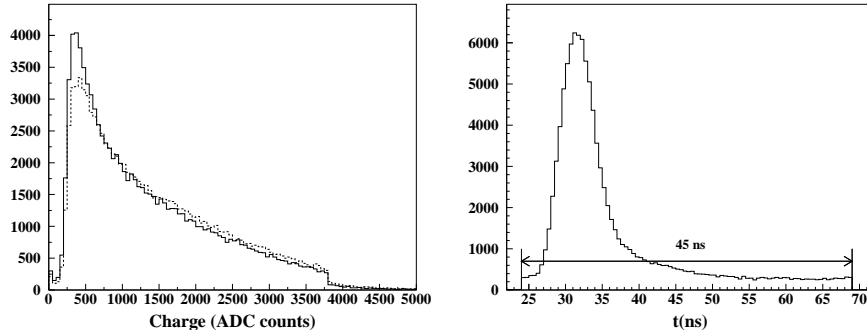


Figure 3: (left) Charge spectrum of side A (solid histogram) and side B (dashed histogram) for the run with a threshold of 36 MeV. (right) Charge weighted time spectrum for the same run. The fixed time width of 45 ns due to the 20 MHz structure of the start signal can be clearly seen.

The value of f_{ICM} depends on the beam shape. We have measured the beam shape in both horizontal (X) and vertical (Y) directions, by using a Beam Profile Monitor (BPM). The BPM consists of two orthogonal hodoscopes, each made of 16 scintillator slabs, 1 cm wide and 0.5 cm thick, readout by Hamamatsu H8711 4×4 multianode PM's through Saint Gobain BCF92 wavelength shifter fibers. The BPM threshold for neutron detection has been estimated to be smaller than 10 MeV equivalent electron energy. The beam profile has been measured at different distances from the collimator exit. The presence of a bulk component pointing to the ${}^7\text{Li}$ target, surrounded by a larger and non pointing halo, has been observed. The X and Y distributions at the position of the calorimeter module are shown in Fig.4: the RMS width of the bulk component is 1.6 cm in X and 1.2 cm in Y, while the halo has a width of about 6 cm in both directions and its center is slightly displaced with respect to the bulk.

The beam shape at the position of the calorimeter has been then parametrized with a bidimensional function reproducing the X and Y distributions of Fig.4 and a value $f_{ICM} = 0.92 \pm 0.03$ has been obtained by integrating that beam shape over the sensitive surface of the calorimeter. The uncertainty takes into account the stability of the measurement with respect to the event selection, and a difference in detection efficiency for bulk and halo neutrons due to their possible different energy composition. Since the bulk neutron distribution is fully contained in the calorimeter sensitive surface the acceptance A is equal to 1.

The overall detection efficiency has been measured for different values of the trigger threshold V_{th} . Table 1 and Fig.5 show the results of the measurement.

The overall uncertainty of about 14% is dominated by the uncertainty on r_{ICM} . The systematic error on the threshold absolute scale due to the uncertainty on the (e/mip) value (see above) has also been considered.

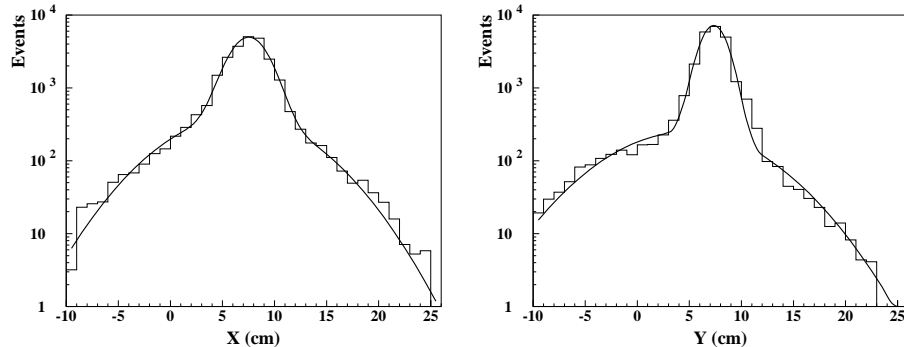


Figure 4: Distribution of the counts in the BPM scintillators in the horizontal (let plot) and vertical (right plot) directions. The curves superimposed are bi-gaussian fits.

Table 1: Results of the measurement: calorimeter rates and beam rates as a function of the central value of the threshold interval. The overall efficiency is evaluated according to eq.(2).

E_{th} (MeV el.eq.)	r_{calo} (kHz)	r_{ICM} (kHz)	ϵ
6	6.64	18.9	0.323
12	4.94	24.9	0.184
18	4.22	26.9	0.144
24	3.53	18.3	0.178
30	3.15	18.9	0.154
36	2.84	18.7	0.140
60	2.27	20.0	0.106
89	1.82	21.1	0.079
119	1.53	25.3	0.056

Table 2 compares the measured overall efficiency with the one obtained in the same beam by a NE-110 bulk scintillator and by the KLOE calorimeter [6].

The three detectors are operated with the same 10 MeV el.eq. threshold and are exposed to the same beam with the spectrum shown in Fig.2¹. Two normalized efficiencies are defined: η_A is the efficiency normalized to the average thickness of active material (to compare with bulk scintillator), η_B is the efficiency normalized to the overall detector thickness.

In order to estimate the kinetic energy dependence of the efficiency we have fit the measured time spectrum shown in Fig.3(b) corresponding to the sample taken with a 36 MeV el.eq. threshold. The fitting function is given by the

¹In the comparison between the KLOE calorimeter and the calorimeter considered in this paper, the different absorber composition has to be considered: 95% Pb - 5% Bi (KLOE) and 32% Pb - 52.5% Bi - 15.5% Sn (this calorimeter).

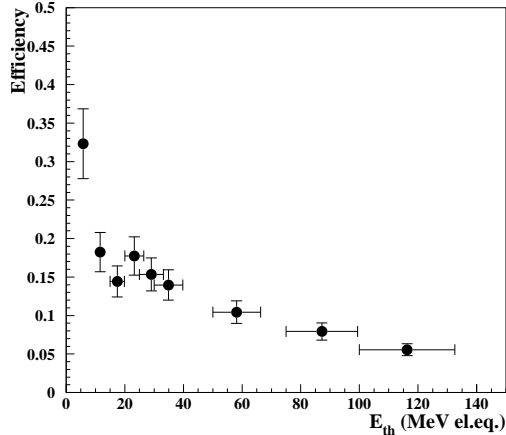


Figure 5: Neutron overall efficiency as a function of the threshold expressed in MeV of electron equivalent for the calorimeter.

Table 2: Overall efficiency per unit of scintillator thickness (η_A) and per unit of overall detector thickness (η_B) for NE-110 bulk scintillator [6], KLOE calorimeter (50% fibers and 50% absorber)[6] and for the calorimeter module (20% fibers and 80% absorber, this work). All measurements have been done for neutrons having the spectrum of Fig.2 and with the same threshold of about 10 MeV.el.eq..

	η_A (%/cm)	η_B (%/cm)
NE-110	0.6	0.6
KLOE	1.9	0.9
this calorimeter	12	2.4

neutron time of flight spectrum obtained from the kinetic energy one shown in Fig.2 through the relation

$$t = \frac{z}{c\sqrt{1 - \left(\frac{M_n}{K_n + M_n}\right)^2}} \quad (3)$$

where $z=510$ cm is the distance of the calorimeter from the proton target, M_n and K_n are the mass and kinetic energy of the neutron respectively.

The spectrum has been convoluted with a time resolution function and multiplied by an efficiency profile $\epsilon(t)$. The time of flight spectrum takes into account the small percentage (of the order of 3%) of rephased low energy neutrons. The time resolution is assumed to be gaussian with a time independent width, and the efficiency is either binned in eight time bins or is parametrized as a 4th order Chebychev polynomial. Free parameters are: the width of the time resolution

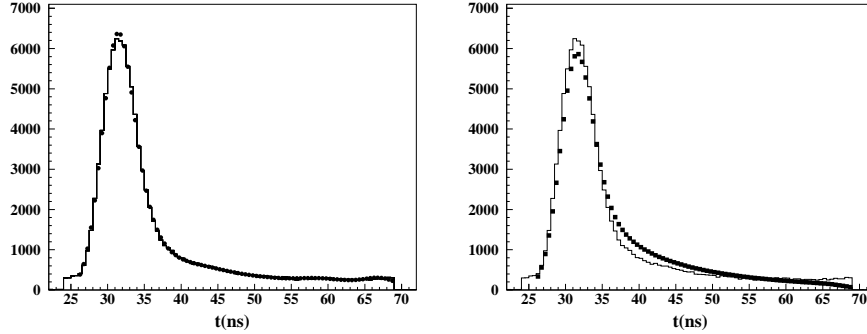


Figure 6: (left) Time spectrum (solid histogram) with superimposed the fit result (points) and (right) the same spectrum with superimposed the expectation in case of uniform efficiency (squares).

and the eight efficiencies or the five coefficients of the Chebychev polynomials. $\epsilon(t)$ is constrained to give an average efficiency equal to the overall efficiency measured as shown above.

Fig.6 shows the experimental spectrum superimposed to the fit result (left plot) and also to the expected one in case of uniform efficiency (right plot). A uniform efficiency in the range 40-180 MeV does not adequately fit the data.

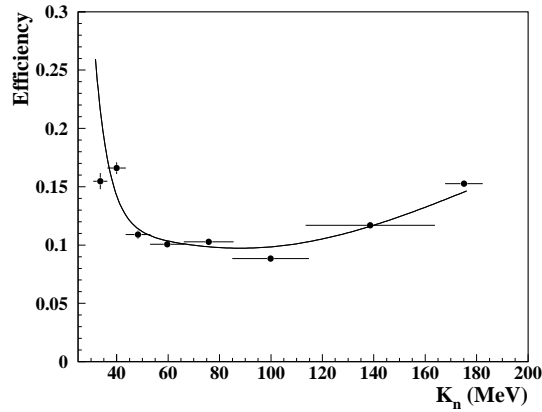


Figure 7: Efficiency resulting from the fit as a function of the neutron kinetic energy K_n : the points are the results for the 8 bins fit and the solid curve the one for the 4th-order Chebychev polynomials.

The efficiency resulting from the fit is expressed as a function of the kinetic energy in Fig.7 both for the binned and for the polynomial fit. A time resolution

value of 2 ns is obtained in both cases. The data indicate an increase of efficiency both at high and low kinetic energies.

5. Conclusions.

The results of the study presented here show that the fraction of passive absorber used in a heterogeneous calorimeter plays an important role in the neutron detection. This also translates in a large enhancement factor with respect to a bulk scintillator detector.

A first indication of an efficiency dependence on the kinetic energy is also obtained.

Acknowledgements. We recall that the calorimeter was built in Rome some years ago with the skilful help of M.Bertino. We thank M.Arpaia, G.Bisogni, A.Cassarà, A.Di Virgilio, U.Martini, A.Olivieri and all the Mechanical LNF Division for the help in the setup of the detector. We also acknowledge M.Rossi for the transportation of the material from LNF to TSL. Moreover we want to warmly thank all the TSL staff for the help during the data taking.

References

- [1] Among the several measurements we quote: C.E.Wiegand et al., Rev.Sci.Instr. 33 (1962) 526 (polystyrene scintillator); D.G.Crabb et al., Nucl.Instr. and Meth.48 (1967) and J.C.Young et al., Nucl.Instr. and Meth.68 (1969) (NE-102 scintillator); G.Betti et al., Nucl.Instr. and Meth. 135 (1976) 307 (NE-110 scintillator).
- [2] A.Ferrari et al., Nucl.Instr. and Meth. A297 (1990) 250; T.Baumann et al., Nucl.Instr. and Meth. B192 (2002) 339.
- [3] F.Ambrosino et al., Eur.Phys.J.C50:(2007) 729-768; see also <http://www.lnf.infn.it/conference/nucleon05/FF/>;
- [4] J.Smeskal et al., Ucl.Phys.A835 (2010) 410; see also http://www.lnf.infn.it/esperimenti/siddharta/LOL_AMADEUS_March2006.pdf.
- [5] M.Adinolfi et al., Nucl.Instr. and Meth. A482 (2002) 364.
- [6] M.Anelli et al., Nucl.Instr. and Meth. A581 (2007) 368; J.Phys.Conf.Ser.160 (2009) 012023.
- [7] R.Wigmans, Nucl.Instr. and Meth. A259 (1987) 398.
- [8] A.Asmone et al., Nucl.Instr. and Meth. A326 (1993) 477; M.Bertino et al., Nucl.Instr. and Meth. A357 (1995) 363.
- [9] D.Acosta et al., Nucl.Instr.and Meth.A320 (1992) 128.
- [10] A.V.Prokofiev et al., Rad.Prot.Dosim. 126 (2007), 18.